Molecular Microbiology (2018) 107(2), 214–228
doi:10.1111/mmi.13878
First published online 11 December 2017

PlpA, a PilZ-like protein, regulates directed motility of the bacterium *Myxococcus xanthus*

Connor B. Pogue, Tianyi Zhou and Beiyan Nan*
Department of Biology, Texas A&M University, College Station, TX 77843, USA.

Summary

The rod-shaped bacterium *Myxococcus xanthus* moves on surfaces along its long cell axis and reverses its moving direction regularly. Current models propose that the asymmetric localization of a Ras-like GTPase, MglA, to leading cell poles determines the moving direction of cells. However, cells are still motile in the mutants where MglA localizes symmetrically, suggesting the existence of additional regulators that control moving direction. In this study, we identified PlpA, a PilZ-like protein that regulates the direction of motility. PlpA and MglA localize into opposite asymmetric patterns. Deletion of the *plpA* gene abolishes the asymmetry of MglA localization, increases the frequency of cellular reversals and leads to severe defects in cell motility. By tracking the movements of single motor particles, we demonstrated that PlpA and MglA co-regulated the direction of gliding motility through direct interactions with the gliding motor. PlpA inhibits the reversal of individual gliding motors while MglA promotes motor reversal. By counteracting MglA near lagging cell poles, PlpA reinforces the polarity axis of MglA and thus stabilizes the direction of motility.

Introduction

Bacterial cells are highly polarized. For rod-shaped bacteria, cell poles constitute important regulatory platforms for a large number of cellular processes including division, differentiation, virulence, chemotaxis and both individual and collective movements (Treuner-Lange and Sogaard-Andersen, 2014; Schumacher and Sogaard-Andersen, 2017). The rod-shaped soil bacterium *Myxococcus xanthus* (*M. xanthus*) features directed motility, regulated pattern formation, biofilm formation and programmed differentiation into fruiting bodies (Muñoz-Dorado *et al.*, 2016). All these functions require the moving direction of cells to be fine tuned in response to environmental and self-generated cues (Zusman *et al.*, 2007; Schumacher and Sogaard-Andersen, 2017). *M. xanthus* lacks flagella and is unable to move by swimming. Instead, *M. xanthus* cells adapt to their natural habitats with two surface motility systems. Social (S-) motility depends on the extrusion and retraction of type IV pili (T4P) at cell poles (Sun *et al.*, 2000; Chang *et al.*, 2016). The motors for gliding motility, also known as adventurous (A-) motility, are proton channels formed by three proteins AglR, AglQ and AglS. This proton channel/motor complex is homologous to the *Escherichia coli* flagella stator complex MotAB (AglR is a MotA homologue while AglQ and AglS are MotB homologues) (Nan *et al.*, 2011; Sun *et al.*, 2011; Nan and Zusman, 2016). The gliding motors in *M. xanthus* move rapidly along helical trajectories, slow down and assemble into multicomponent gliding complexes at the putative focal adhesion sites, and propagate proton motive force onto the cell surface (Nan *et al.*, 2010b, 2011, 2013, 2014; Luciano *et al.*, 2011; Sun *et al.*, 2011; Faure *et al.*, 2016; Nan and Zusman, 2016). *M. xanthus* coordinates both motility systems to move unidirectionally along the long cell axis (Lenz and Sogaard-Andersen, 2011; Kaimer *et al.*, 2012). To achieve optimal motility efficiency, cells reverse their moving direction regularly and control the reversal frequency in a narrow range (Wu *et al.*, 2009). Fixed moving direction, such as in the hypo-reversing *frz* null mutants, impairs the efficiency of colony expansion. Similarly, mutants reversing their moving direction at high frequency (hyper-reversing) also show severe motility defects (Bustamante *et al.*, 2004). In laboratory, S-motility is predominant on soft surfaces (such as 0.3%–0.5% agar) and plays a major role in the collective movements of cell groups. In contrast, A-motility functions poorly on soft surfaces due to its abnormally high reversal frequencies (Zhou and Nan, 2017). Instead, A-motility is more efficient on harder surfaces (such as 1.5%–2.0% agar) and contributes more for the movements of individual cells (Shi and Zusman, 1993; Zhou and Nan, 2017).

Accepted 7 November, 2017. *For correspondence. E-mail bnan@tamu.edu; Tel. 979-845-3487; Fax 979-845-2891.

M. xanthus cells determine their moving direction through small GTPases and cytoskeletal elements (Leonardy *et al.*, 2010; Mauriello *et al.*, 2010; Zhang *et al.*, 2010; Lenz and Sogaard-Andersen, 2011; Treuner-Lange and Sogaard-Andersen, 2014; Nan *et al.*, 2015; Treuner-Lange *et al.*, 2015). The central regulator is MglA, a bacterial homologue of the Ras-family GTPases. During movement, GTP-bound MglA localizes in an asymmetric gradient and forms major clusters at the leading cell poles (Leonardy *et al.*, 2010; Zhang *et al.*, 2010; Nan *et al.*, 2015). Although the molecular mechanism is unclear, MglA was observed to determine the direction of S-motility by sorting PilB and PilT, the T4P motor ATPases, to opposite cell poles (Bulyha *et al.*, 2013). For A-motility, MglA may control the moving direction of individual motors through direct interaction (Nan *et al.*, 2015), or, alternatively, facilitate the assembly and reassembly of the gliding complexes to the MreB cytoskeleton (Treuner-Lange *et al.*, 2015). Although these two hypotheses emphasize different aspects, they might point to the same molecular mechanism: MglA determines the moving direction of cells by regulating the movements of individual motor complexes.

The GTPase activity of *M. xanthus* MglA is regulated by its cognate GTPase-activating protein (GAP), MglB. MglB localizes into an asymmetric pattern opposite to MglA, forming major clusters at lagging cell poles. MglB activates the GTPase activity of MglA, expelling MglA-GTP from lagging cell poles (Leonardy *et al.*, 2010; Zhang *et al.*, 2010; Lenz and Sogaard-Andersen, 2011; Miertzschke *et al.*, 2011). RomR, a response regulator, reinforces the MglA polarity axis through interactions with both MglA and MglB (Leonardy *et al.*, 2007; Keilberg *et al.*, 2012; Zhang *et al.*, 2012; Kaimer and Zusman, 2013; Kaimer and Zusman, 2016). MglC, a recently identified orphan paralogue of MglB, also modulates the moving direction of cells through an unknown mechanism (McLoon *et al.*, 2015). Cells reverse their direction of movement when the Frz system, a master chemosensory pathway, inverts the asymmetric localization of MglA, MglB and RomR (Leonardy *et al.*, 2010, Zhang *et al.*, 2010, Keilberg *et al.*, 2012, Zhang *et al.*, 2012; Kaimer and Zusman, 2013; Kaimer and Zusman, 2016). However, signals from outside of the Frz-Mgl circuit, such as extracellular polysaccharides, also regulate cellular reversal (Zhou and Nan, 2017).

MglA localizes symmetrically at both cell poles in the absence of MglB. However, Δ*mglB* cells are still motile, albeit reverse twice as frequently as the wild type cells, suggesting the existence of additional regulators that maintain the directed motility of cells (Leonardy *et al.*, 2010; Zhang *et al.*, 2010). In this study, we identified such a regulator, PlpA, a PilZ-like protein. In wild type cells, PlpA and MglA localize into opposite asymmetric patterns. While MglA interacts with AglR, the MotA homologue in the gliding motor (Nan *et al.*, 2015), PlpA interacts with AglS, a MotB homologue. The correct localization of MglA and MglB depends on PlpA and PlpA depends on MglB and MglC. By studying the behavior of single motors using single-particle microscopy, we found that PlpA antagonized MglA by inhibiting the reversal of individual gilding motors. Based on these results, we propose that PlpA is a novel regulator that stabilizes the moving direction of cells by antagonizing MglA at lagging cell poles.

Results

PlpA (MXAN_2528) interacts with AglS in the gliding motor

We identified PlpA in a bacterial adenylate cyclase two-hybrid (BACTH) (Karimova *et al.*, 1998) screen for proteins that potentially interact with the AglRQS gliding motor. DNA fragments from an open reading frame (ORF), *mxan_2528*, were repeatedly identified when using *aglS*, the gene encoding one of the two MotB homologues in the motor complex, as the bait (see Materials and Methods). To confirm this interaction, we fused the motor genes, *aglR* and *aglS* and the *mxan_2528* ORF to the 5' ends of the DNA sequences that encode complementary fragments of adenylate cyclase (CyaA) and expressed the fusion proteins. Protein interactions can be determined by the blue color of colonies associated with β-galactosidase activity (Karimova *et al.*, 1998). As shown in Fig. 1A, MXAN_2528 directly interacts with the MotB homologue AglS, but not with the MotA homologue AglR. Consistent with previous report (Nan *et al.*, 2015), AglR displayed strong self-interaction and directly interacted with AglS. AglQ, the other MotB homologue, did not show any interaction with AglR and AglS in BACTH assay even though AglRQS presumably form a transmembrane channel (Sun *et al.*, 2011) (Supporting Information Fig. S1). We speculated that our BACTH constructs of AglQ-Cya^{T18} and AglQ-Cya^{T25} might not express or fold correctly in *E. coli* cells and, therefore, did not include AglQ in further BACTH studies.

PlpA (MXAN_2528) regulates the reversal frequency of M. xanthus *cells*

The *mxan_2528* ORF encodes a putative cytoplasmic PilZ-like (pfam07238) protein of 132 amino acids (Fig. 1B), which is conserved in many species in the order of *Myxococcales* (Supporting Information Fig. S2). According

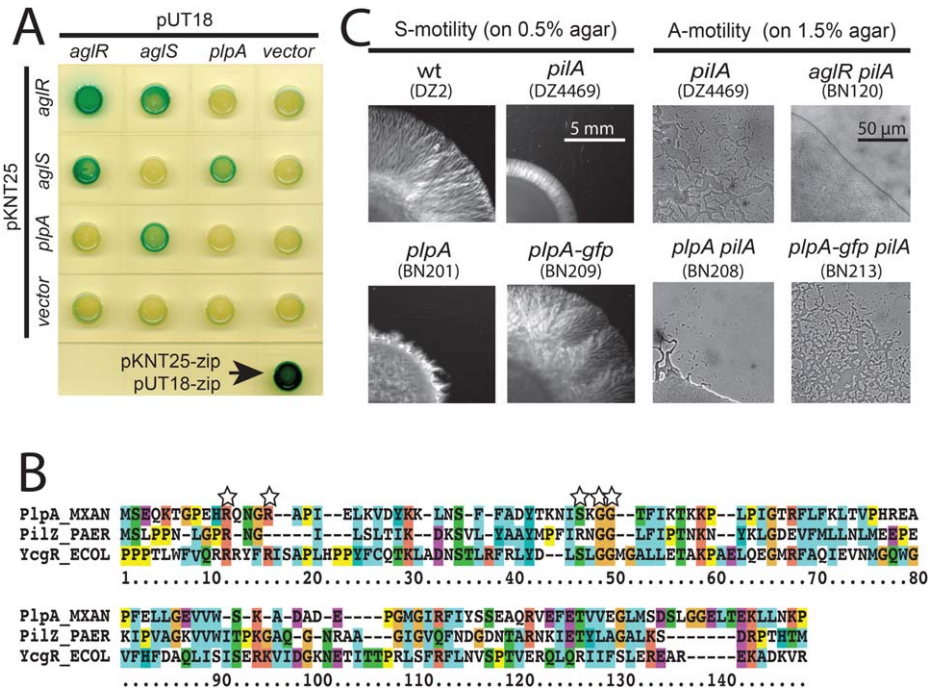

Fig. 1. PlpA (MXAN_2528) regulates both A- and S-motility in *M. xanthus*.
A. Bacterial two-hybrid (BACTH) assay shows that PlpA directly interacts with AglS, the MotB homologue in the gliding motor. The gene encoding the leucine zipper region of the yeast GCN4 protein (*zip*) and empty vectors were used as positive and negative controls respectively.
B. PlpA regulates both S- and A-motility systems, which were assayed on 0.5% and 1.5% agar surfaces respectively.
C. Sequence alignment between *M. xanthus* PlpA (PlpA_MXAN), *Pseudomonas aeruginosa* PilZ (PilZ_PAER) and *E. coil* YcgR (YcgR_ECOL) showing the c-di-GMP binding motif. Key residues required for c-di-GMP binding in *E. coli* YcgR (Ryjenkov *et al.*, 2006) are marked by stars.

to recent transcriptome analyses, this ORF is constitutively transcribed in *M. xanthus* cells (Muller *et al.*, 2010; Huntley *et al.*, 2011). We named MXAN_2528, the PilZ-like protein, PlpA. To investigate the function of this protein, we constructed an in-frame deletion of the entire *plpA* ORF. We assayed S-motility of this strain on a 0.5% agar surface, where the contribution of gliding motility to colony expansion is negligible (Shi and Zusman, 1993). The Δ*plpA* colonies expanded from the initial inoculum on 0.5% agar, indicating that T4P in this strain were still functional. However, the migration of the Δ*plpA* colonies after 24 h incubation was reduced to less than 50% of the wild type (DZ2) level, indicating a severe defect in S-motility (Fig. 1C). We then completely eliminated S-motility in the Δ*plpA* strain by disrupting pilus production with a *pilA::tet* insertion. The resulted strain was also defective in A-motility, as the colony diameters on 1.5% agar were reduced to 60% of the *pilA*$^-$ level (Fig. 1C). Despite to its defects in motility, the Δ*plpA* cells still formed fruiting bodies on CF agar (Supporting Information Fig. S3). Taken together, motility assays indicate that PlpA is a regulator for both A- and S-motility systems.

The phenotypes caused by the *plpA* deletion were striking, because most of the genes required for motility in *M. xanthus* function in only one of the motility systems, except for *mglA*, *mglB* and *romR*, which are essential for both motility systems (Hodgkin and Kaiser, 1979; Leonardy *et al.*, 2010; Mauriello *et al.*, 2010; Zhang *et al.*, 2010; Keilberg *et al.*, 2012; Zhang *et al.*, 2012). While the Δ*mglA* cells are nonmotile, Δ*mglB* and Δ*romR* cells show both motility defects and hyper-reversing phenotypes (Leonardy *et al.*, 2007; Leonardy *et al.*, 2010; Zhang *et al.*, 2010; Keilberg *et al.*, 2012). To test if the motility defects of the Δ*plpA* cells were also due to abnormal cellular reversals, we, therefore, calculated the reversal frequency of the Δ*plpA* cells on the surface of 1.5% agar, where both A- and S-motility systems were functional (Shi and Zusman, 1993). As shown in Fig. 2, comparing to the wild type cells that reversed their moving direction once every 7.69 min (average reversal frequency 0.13 ± 0.01 min^{-1}, mean ± SD, $n = 40$, same below), the Δ*plpA* cells hyper-reversed (once every 3.39 min, 0.30 ± 0.01 min^{-1}). To determine whether enhanced activity of PlpA might reduce the reversal frequency of cells, we constructed a strain where the *plpA* gene was expressed both from its endogenous locus and at a different locus from a vanillate-inducible promoter (p_{van}) (Iniesta *et al.*, 2012). In the presence of 200 μM sodium vanillate, reversal frequency of the cells overexpressing PlpA was significantly reduced, to once every 52 min (0.02 ± 0.00 min^{-1}), similar to the reversal frequency of the hyper-reversing *frzE* cells (0.02 ± 0.01 min^{-1}) (Fig. 2). Accordingly, *frzE* cells and the cells overexpressing PlpA displayed similar colony expansion patterns (Supporting Information Fig. S4). As a control, in wild type cells, the presence of 200 μM sodium vanillate did not affect S-motility or change their reversal frequency. The potential leaky expression of PlpA under the control of p_{van} in the absence of sodium vanillate did not affect either

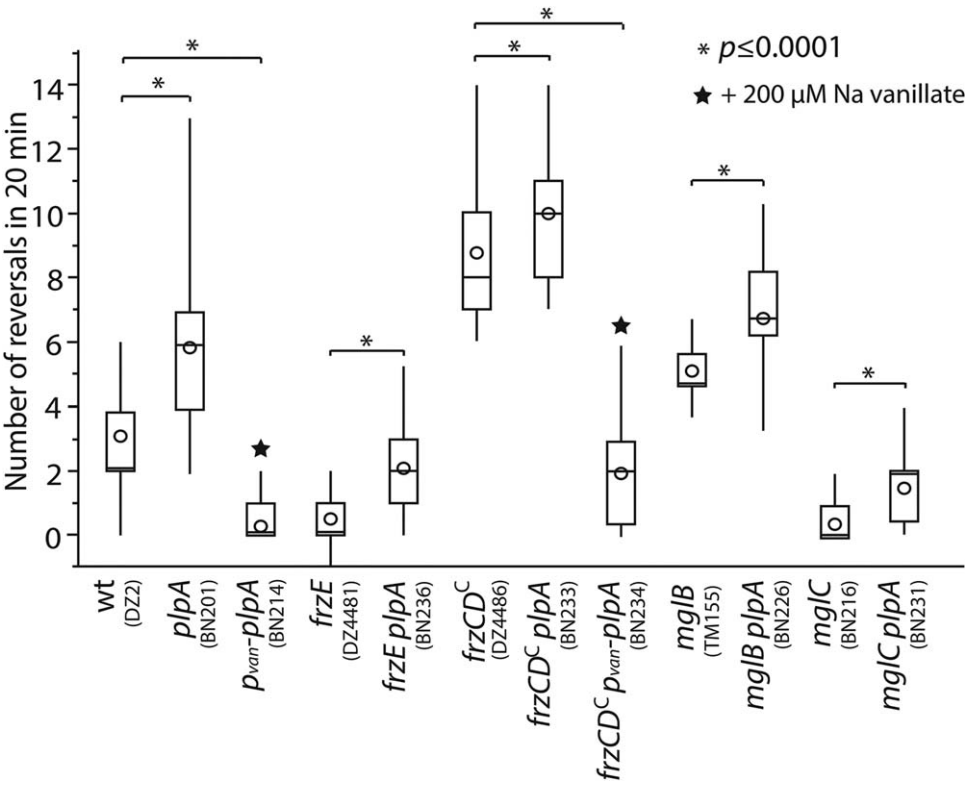

Fig. 2. PlpA inhibits cellular reversal. For each strain, the reversals of 40 cells on 1.5% agar (0.5 CTT) within 20 min were shown in a box plot. The central rectangle of each box plot spans the second and third quartile, while the whiskers above and below the box show the minimum and maximum. The circles mark the average reversal numbers per cell in 20 min, whereas the bars inside boxes annotate the median reversal numbers. *p* values were calculated using the Student paired *t* test with a two-tailed distribution (same below).

S-motility or cellular reversal (Supporting Information Fig. S5).

As we reported previously, the wild-type cells that moved with both A- and S-motility reversed significantly more frequently than the cells that moved with only A- or S-motility (Zhou and Nan, 2017). This result suggested that the reversal of one motility system could trigger the reversal of the other motility system and subsequently, cellular reversal. Similarly, recent studies suggested that the Frz system might regulate the two motility systems differently (Guzzo *et al.*, 2015; Kaimer and Zusman, 2016). To test if PlpA inhibits the reversal of both A- and S-motility, we calculated the reversal frequencies of the *plpA pilA* (moving with A-motility only) and *plpA aglQS* (moving with S-motility only) double mutants on 1.5% agar. As shown in Supporting Information Fig. S6, the introduction of an additional *plpA* deletion increased the reversal frequencies of both the *pilA* and *aglQR* (genes encoding both the MotB homologues were deleted) cells. Taken together, cellular reversal assays indicated that PlpA inhibits the cellular reversals in both A- and S-motility.

PlpA regulates cellular reversals together with the Frz-Mgl pathway

The Frz chemosensory pathway has been shown as a master system that controls cellular reversals through RomR and the Mgl module (Kaimer and Zusman, 2013; Kaimer and Zusman, 2016). To determine whether PlpA also functions within the Frz-Mgl pathway, we created double mutants by deleting the *plpA* gene in the Δ*frzE*, *frzCD*^{c} (*frzCD*$^{\Delta 6-153}$), Δ*romR*, Δ*mglA*, Δ*mglB* and Δ*mglC* strains. As shown in Supporting Information Fig. S4, it was difficult to find conclusive genetic evidence for an epistatic relationship between PlpA and the Frz-Mgl pathway solely based on either S- or A-motility. For example, the S-motility spreading of the Δ*frzE* Δ*plpA* and Δ*romR* Δ*plpA* double mutants on 0.5% agar surfaces appeared similar to that of the Δ*plpA* single mutant, suggesting that PlpA might function downstream of both the Frz pathway and RomR (Supporting Information Fig. S4A). However, on 1.5% agar surfaces, gliding efficiencies of these double mutants were similar to that of the Δ*frzE* and Δ*romR* strains respectively, suggesting that PlpA might function upstream of both the Frz pathway and RomR (Supporting Information Fig. S4B).

Since the Δ*plpA* deletion causes cells to hyper-reverse, we decided to calculate the reversal frequencies of the above single and double mutants. Consistent with previous reports (Leonardy *et al.*, 2007; Leonardy *et al.*, 2010; Zhang *et al.*, 2010, 2012; Keilberg *et al.*, 2012; McLoon *et al.*, 2015), Δ*frzE* and Δ*mglC* cells reversed their polarity at very low frequencies (once every 32–34 min, 0.02 ± 0.01 min^{-1}, hypo-reversing), while the *frzCD*^{c} and Δ*mglB* cells hyper-reversed (once

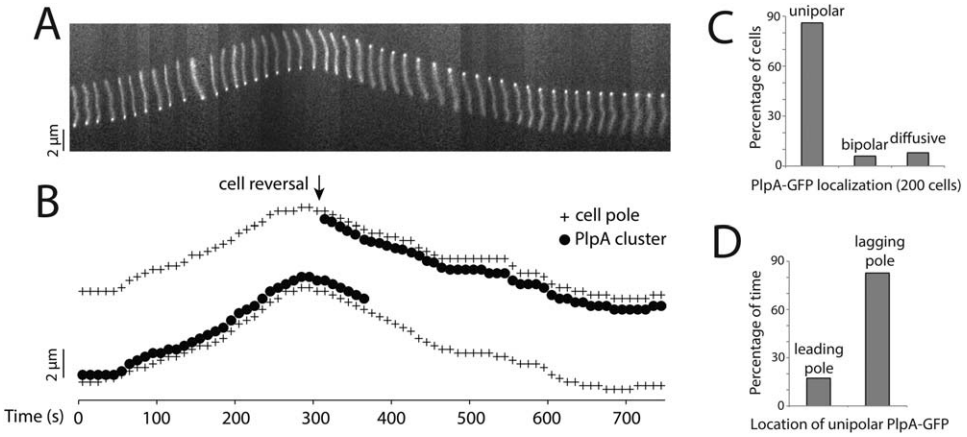

Fig. 3. PlpA-GFP localizes at lagging cell poles and switch polarity as cells reverse.
A. PlpA-GFP localizes at lagging cell poles and switches polarity as cell reverses. Fluorescence signals were recorded in 10-s time intervals.
B. The positions of PlpA-GFP clusters and cell poles were plotted frame-by-frame.
C. Among the 200 cells we studied, 86% showed that PlpA-GFP formed bright clusters at single cell poles.
D. Frame-by-frame analysis on 64 moving cells that displayed unipolar PlpA clusters. Among 6464 frames analyzed (101 frames per cell), PlpA localized at lagging cell poles in 82.7% frames.

every 2.3 min, 0.44 ± 0.01 min^{-1} and once every 4.1 min, 0.20 ± 0.01 min^{-1} respectively) (Fig. 2). The Δ*frzE* Δ*plpA* and Δ*mglC* Δ*plpA* double mutants reversed cell polarity 277% and 160% more frequently than the Δ*frzE* and Δ*mglC* single mutants respectively. To our surprise, deletion of the *plpA* gene further increased the reversal frequencies of the hyper-reversing *frzCD*^{c} and Δ*mglB* cells by 13% and 32% respectively (Fig. 2). Compared to the Δ*mglB* cells that move for one cell length before reversing (Zhang *et al.*, 2010), cells carrying the *plpA mglB* double deletion showed even smaller displacements between reversals (0.5 ± 0.2 cell length). The introduction of the *plpA* deletion increased the reversal frequencies of cells in both hypo- and hyper-reversing backgrounds compared to the parental strains (Fig. 2). Strikingly, overexpressing PlpA in the presence of 200 μM sodium vanillate in the hyper-reversing *frzCD*^{c} background reduced cellular reversal frequency to once every 10.2 min (0.10 ± 0.01 min^{-1}) (Fig. 2). As a result, motility defects of *frzCD*^{c} cells were partially rescued by excessive PlpA (Supporting Information Fig. S4). Thus, rather than functioning in the same signaling cascade, PlpA and the Frz-Mgl pathway regulate cell reversals in an additive manner. We were not able to calculate the reversal frequencies of the Δ*romR*, Δ*mglA*, Δ*romR* Δ*plpA* and Δ*mglA* Δ*plpA* cells because individual cells of these mutants did not show significant movements (Supporting Information Fig. S4B).

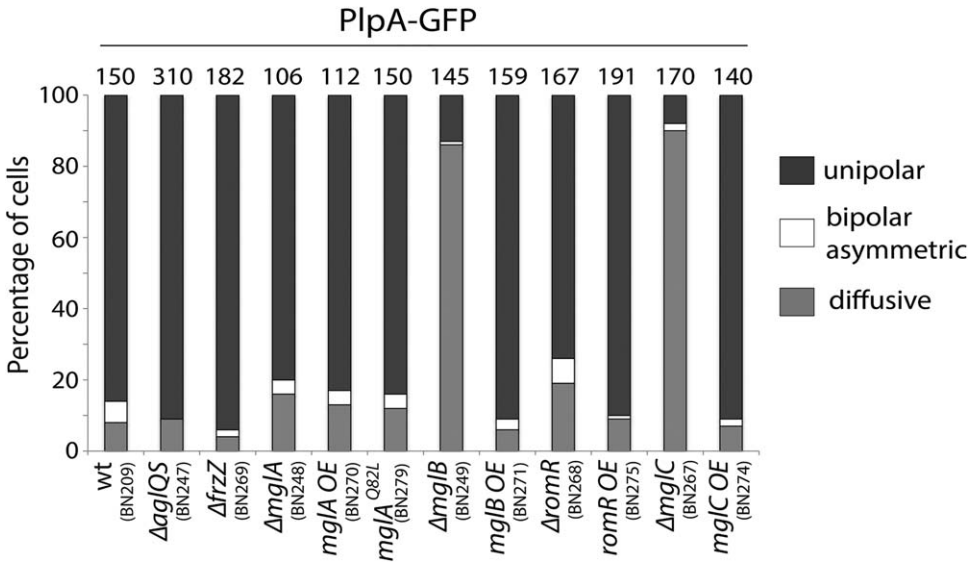

Fig. 4. The unipolar localization of PlpA-GFP clusters depends on MglB and MglC. The percentage of cells harboring unipolar and bipolar asymmetric PlpA-GFP clusters and diffusive fluorescence signals are shown in different genetic backgrounds. Overexpression (OE) of proteins was achieved using a vanillate-inducible promoter in the presence of 200 μM sodium vanillate. For each strain, the total number of cells calculated is shown on top of the bar.

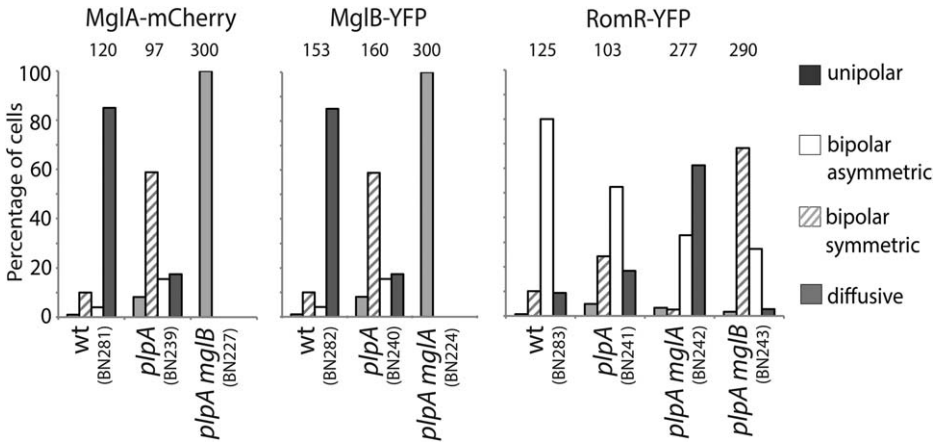

Fig. 5. PlpA regulates the localization of both MglA and MglB. The localization of MglA, MglB and RomR was tested in wild type and various genetic backgrounds that contain *plpA* deletion. For each strain, the total number of cells calculated is shown on top of the bars. MglA-mCherry and RomR-YFP were expressed in the presence of 10 μM sodium vanillate.

PlpA localizes in an asymmetric pattern and concentrates at lagging cell poles

To further study its function, we expressed PlpA with a GFP label at its C-terminus as the sole source of PlpA under its native genetic control. This strain showed phenotypes in A- and S-motility that were indistinguishable from the wild type (Fig. 1C), indicating that the PlpA-GFP fusion is fully functional. Using regular fluorescence microscopy, we studied the localization of PlpA-GFP in live cells. As shown in Fig. 3A and B, PlpA localizes along the cell bodies and aggregates into bright clusters at the lagging cell poles. Importantly, the bright PlpA clusters re-localized to the new lagging poles when cells reversed their moving direction, indicating that the asymmetric localization pattern of PlpA inverted coordinately with cell reversals (Fig. 3A and B). We recorded the dynamics of PlpA-GFP clusters in 200 moving cells. We found that 172 cells (86%) contained PlpA-GFP clusters at single cell poles, while 20 (10%) and 8 (4%) cells showed diffusive and asymmetric bipolar localization patterns respectively (Fig. 3C). We noticed that in many cases, PlpA localized to bipolar patterns transiently during cell reversals (between 300 s and 400 s in Fig. 3B). To further quantify the localization of PlpA, we performed frame-by-frame analysis on 64 moving cells that displayed unipolar PlpA clusters. Among 6464 frames analyzed (101 frames per cell, at 10-s intervals), we found that PlpA localized to lagging cell poles in 82.7% frames (Fig. 3D). Taken together, our data indicated that PlpA localizes to lagging cell poles and switches to new lagging poles as cells reverse.

The asymmetric localization of PlpA requires MglB and MglC

To determine how the asymmetric localization of PlpA is regulated, we expressed PlpA-GFP in various genetic backgrounds. While PlpA-GFP localized at lagging cell poles in near 90% of cells (Figs. 3 and 4), it became largely diffusive when *mglB* and *mglC* were deleted (Fig. 4). In contrast, PlpA-GFP still concentrated at the lagging cell poles in Δ*aglQS*, Δ*frzZ*, *mglA* overexpression (*mglA OE*), MglA constitutively active (*mglA*^{Q82L}), *mglB* overexpression (*mglB OE*), Δ*romR*, *romR* overexpression (*romR OE*) and *mglC* over expression (*mglC OE*) backgrounds (Fig. 4). It was not possible to identify the leading poles of the Δ*romR* and Δ*mglA* cells since both strains did not move. However, PlpA still maintained asymmetric localization pattern in Δ*romR* and Δ*mglA* cells where it formed a bright cluster at only one pole in each cell (Fig. 4). Taken together, the asymmetric localization of PlpA depends on both MglB and MglC.

Similar to PlpA, MglB and MglC also localize into asymmetric patterns and concentrate at lagging cell poles (Leonardy *et al.*, 2010; Zhang *et al.*, 2010). To investigate if PlpA interacts with MglB, MglC and other key proteins in the Frz-Mgl pathway, we performed pairwise BACTH assays between PlpA and FrzZ, RomR, MglA, MglB and MglC. As shown in Supporting Information Fig. S7, we did not observe any interaction between PlpA and these Frz-Mgl proteins.

PlpA regulates the polar localization of the MglAB module

To investigate whether PlpA regulates the localization of the regulators in the Frz-Mgl pathway, including FrzZ, RomR, MglA, MglB and MglC, we labeled these proteins with fluorescence tags and studied their localization in wild type and Δ*plpA* backgrounds using fluorescence microscopy. While displaying unipolar localization patterns in wild type background, both MglA and MglB localized into bipolar patterns in the absence of PlpA. Thus, although MglA and MglB do not require the function of PlpA to localize to cell poles, they do depend on

PlpA to localize into unipolar patterns (Fig. 5). We further studied the localization of MglA and MglB in the *plpA mglB* and *plpA mglA* double deletion strains respectively. Our data showed that MglA and MglB diffused in these double mutants and lost polar localization completely.

To test if PlpA regulates the polar localization of RomR, we investigated the localization of RomR-YFP in the *plpA* deletion strain. As shown in Fig. 5, RomR largely retained its asymmetric bipolar localization pattern in the absence of PlpA but slightly switched toward symmetric bipolar (Fig. 5). We further imaged RomR-YFP in the *plpA mglB* and *plpA mglA* double deletion strains. In the *plpA mglB* double deletion strain, RomR switched to symmetric bipolar localization (Fig. 5), similar to its localization pattern in the *mglB* single deletion background (Keilberg *et al*., 2012). Similar to the observation in the *mglA* single deletion background (Keilberg *et al*., 2012), PlpA predominantly to single cell poles (Fig. 5). Thus, our data indicated that PlpA does not regulate the polarity of RomR directly. In addition, the deletion of *plpA* alone does not affect the localization of neither FrzZ nor MglC (Supporting Information Fig. S8). Taken together, although its molecular mechanism is still unclear, our data suggested that the mutual dependence between PlpA and the MglAB module determines the polarity axes of cells.

The regulatory function of PlpA does not require cyclic-di-GMP (c-di-GMP)

PlpA belongs to the PilZ protein family. Many proteins containing the PilZ domains are receptors of c-di-GMP, a second messenger that regulates multiple functions in bacteria, especially motility and biofilm formation (Amikam and Galperin, 2006; Jenal and Malone, 2006; Ryjenkov *et al*., 2006; Hengge, 2009). In *M. xanthus*, c-di-GMP regulates the T4P-dependent S-motility and sporulation (Skotnicka *et al*., 2016a, 2016b). As shown in Fig. 1C and Supporting Information Fig. S2, PlpA contains the signature c-di-GMP binding motif RxxxR-$N_{20–30}$-D/NxSxgG (Amikam and Galperin, 2006; Ryjenkov *et al*., 2006). Mutations on key residues in the c-di-GMP binding motif of the *Escherichia coli* YcgR protein resulted in significant motility defects (Ryjenkov *et al*., 2006). To investigate if c-di-GMP is required for the regulatory function of PlpA, we constructed three point mutations on PlpA using site-directed mutagenesis: an R to D mutation on residue 15 (R15D), an S to A mutation on residue 39 (S39A) and G to A mutations on residues 41 and 42 (G41A G42A) (Supporting Information Fig. S9A). To our surprise, all three strains that expressed these PlpA mutants as the sole sources of PlpA retained both S- and A-motility at the wild type level (Supporting Information Fig. S9B). We further determined the reversal frequencies of these cells. Consistent with their phonotypes in motility, cells of wild type and the three mutant strains all reversed at similar frequencies (Supporting Information Fig. S9C). Moreover, we labeled all three PlpA mutants with GFP and expressed them as the sole sources of PlpA. As shown in Supporting Information Fig. S9D, the majority of the GFP-labeled PlpA mutants still localized at lagging cell poles, indicating that these point mutations did not affect the localization of PlpA.

To investigate if PlpA binds to c-di-GMP *in vitro*, we expressed PlpA in *E. coli* with a 6 × His tag on its N-terminus and purified the recombinant protein using Ni^{2+} affinity chromatography. To eliminate the potentially prebound c-di-GMP, an aliquot of purified PlpA was denatured using 4 M urea and refolded on a nickel column. We then performed isothermal titration calorimetry (ITC) assay, using c-di-GMP as titrant. As shown in Supporting Information Fig. S10, the injection of c-di-GMP into purified PlpA solution (10 μM), purified and refolded PlpA solution (10 μM) and the buffer control caused identical patterns of thermodynamic changes. Thus, we did not detect any binding between PlpA and c-di-GMP *in vitro*. The fact that PlpA contains the intact c-di-GMP binding motif suggests that PlpA might bind to c-di-GMP or other nucleotides, such as cyclic AMP-GMP *in vivo* (Hallberg *et al*., 2016). However, our data provide strong evidence that c-di-GMP is not required for the regulatory function of PlpA on motility.

PlpA does not influence the localization of FrzS, a regulator for S-motility

PilZ is essential for the assembly of T4P in *Pseudomonas aeruginosa* (Alm *et al*., 1996). However, the structure of the *M. xanthus* T4P machinery does not suggest a PilZ module (Chang *et al*., 2016). Moreover, S-motility is still functional in the Δ*plpA* strain (Fig. 2 and Supporting Information Fig. S4), indicating that PlpA is not essential for T4P assembly in *M. xanthus*. We labeled FrzS, a regulator of S-motility, with GFP in both the wild type and the Δ*plpA* backgrounds. In both strains, FrzS localizes asymmetrically at both cell poles, with brighter clusters at leading poles (Supporting Information Fig. S11A). These data indicate that PlpA might not regulate the polarity of S-motility through FrzS. Moreover, we did not detect any interaction between PlpA and FrzS (Supporting Information Fig. S11B). We further performed pairwise BACTH assays to probe interactions between PlpA and the proteins exposed to the cytoplasm in the T4P, including

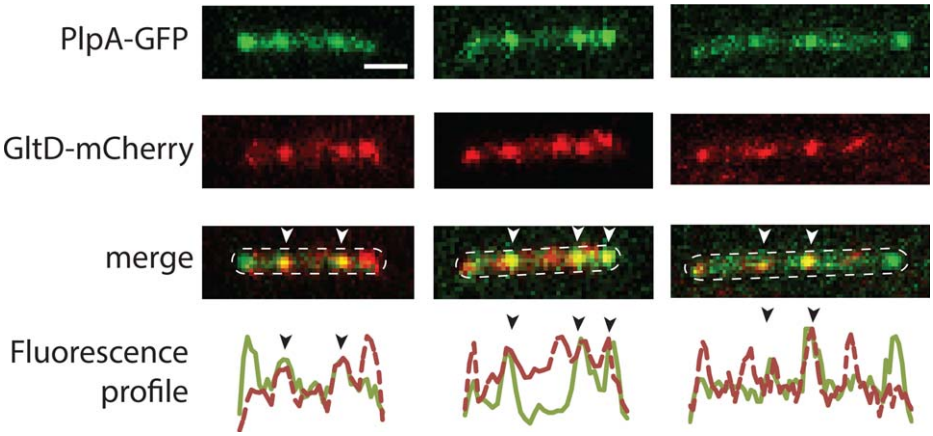

Fig. 6. PlpA assembles into the gliding machinery. The clusters of GltD (AgmU)-mCherry indicate the FACs sites where motility proteins assemble into gliding machineries. The localization of PlpA-GFP and GltD-mCherry was shown in three representative cells. The lower panels show the fluorescence profiles of both proteins. White arrows point to the locations where PlpA and GltD co-localize. Scale bar, 1 μm.

PilB, PilT, PilC and PilM (Berleman *et al.*, 2011). Shown in Supporting Information Fig. S11B, no interaction was detected between PlpA and these targets. Taken together, the mechanism by which PlpA regulates the polarity of S-motility remains to be investigated.

PlpA co-localizes with the gliding machinery

Strikingly similarity to MglA (Nan *et al.*, 2015; Treuner-Lange *et al.*, 2015), PlpA directly interacts with the motor of gliding motility (Fig. 1). MglA predominantly localizes to single (leading) cell poles, whereas its constitutively active variant, MglA^{Q82A}, localizes both to

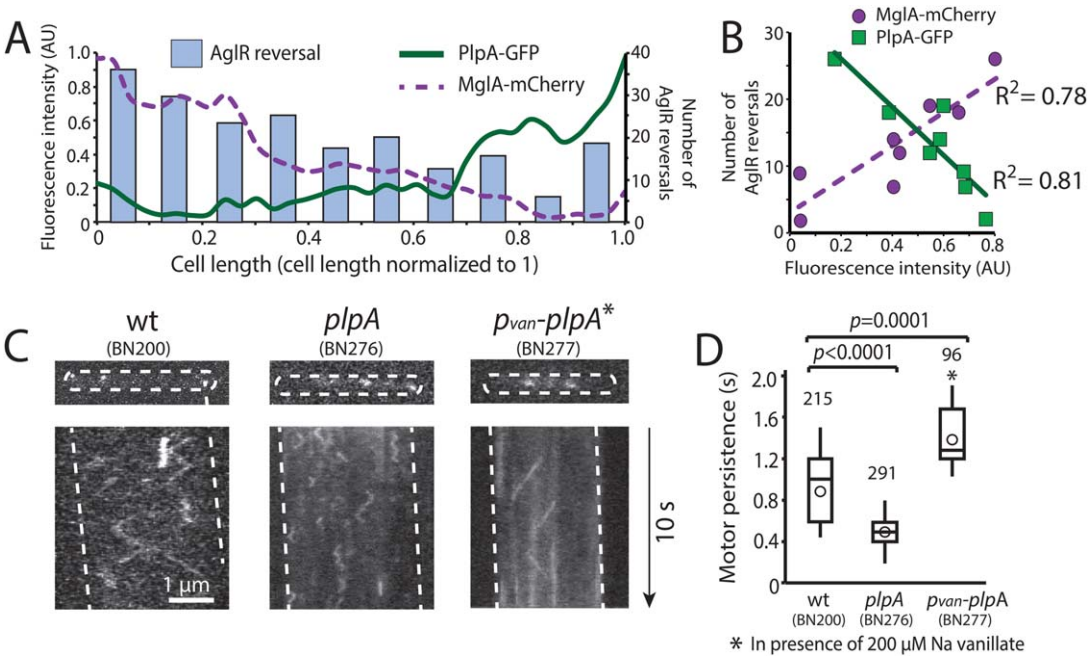

Fig. 7. PlpA inhibits the reversal of individual gliding motors.
A. Average of 20 cells showed that PlpA-GFP (solid green line) and MglA-mCherry (dashed purple line) formed opposite gradients along cell bodies. The maximum fluorescence intensity of each protein in each cell is normalized as 1. The behavior of individual gliding motors was visualized by tracking the dynamics of AglR-PAmCherry particles. The length of each cell was normalized as 1 and divided into 10 sections, and the number of reversals of AglR particles in each section was plotted as blue bars.
B. The spatial distribution of AglR reversals is positively correlated with MglA concentration and negatively correlated with PlpA concentration. The number of AglR reversals in each section of cell was plotted as a function of the fluorescence intensity of PlpA-GFP (green square) and MglA-mCherry (purple dot) in the same section.
C. Kymographs of AglR-PAmCherry particles in 10-s time periods in wild type (wt), Δ*plpA* and *plpA* overexpression cells.
D. Quantitative analysis of motor persistence (the time each AglR-PAmCherry particle traveled before reversing). Comparing to the wild type cells, AglR-PAmCherry particles reversed their moving direction at elevated frequencies in the Δ*plpA* cells but rarely reversed in the cells overexpressing *plpA*. For each strain, the total number of AglR particles tracked is shown on top of the bars.

cell poles and one of the putative 'focal adhesion' complexes (FACs) where the gliding machinery assembles (Zhang *et al*., 2010; Miertzschke *et al*., 2011; Treuner-Lange *et al*., 2015). It is possible that PlpA also assembles into the gliding machinery. To test this hypothesis, we labeled PlpA with GFP and GltD (AgmU), a core protein that assembles into the gliding machinery (Nan *et al*., 2010b; Luciano *et al*., 2011; Faure *et al*., 2016), with mCherry and investigated their localization using fluorescence microscopy. As shown in Fig. 3, PlpA-GFP diffuses along cell bodies and concentrates into bright clusters at lagging cell poles. After examining 382 cells carefully, we were able to detect nonpolar clusters of PlpA-GFP in 18 (4.7%) cells (Fig. 6). Without exception, all these clusters co-localized with GltD-mCherry at the FACs (Fig. 6). Taken together, our data indicate that similar to MglA, a subpopulation of PlpA assembles into the gliding machinery.

PlpA antagonizes MglA in regulating the dynamics of the gliding motors

For gliding motility, individual motors can move and reverse independently (Nan *et al*., 2013, 2015). MglA promotes the reversal of individual gliding motors and the spatial distribution of motor reversals correlates with the concentration gradient of MglA positively (Nan *et al*., 2015). Since PlpA and MglA show opposite localization patterns and both interact with the gliding motors, we hypothesized that both proteins might regulate cell polarity though motor complexes.

To measure the local concentrations of MglA and PlpA precisely, we expressed MglA-mCherry and PlpA-GFP simultaneously and scanned their fluorescence signals along long cell axes. Consistent with our previous report, as the distance from the leading cell poles increased, the fluorescence intensities of MglA-YFP decreased gradually (Nan *et al*., 2015) (Fig. 7A). In contrast, the intensities of PlpA increased gradually toward the lagging cell poles (Fig. 7A). To quantify the concentration of both proteins, we averaged the intensities of each protein in 20 cells, with cell lengths normalized to 1. The results showed that MglA and PlpA formed opposite gradients along cell bodies (Fig. 7A).

To investigate if PlpA regulates the movements of individual gliding motors, we labeled AglR, the MotA homologue in the gliding motor, with photoactivatable mCherry (PAmCherry). Previously we showed that gliding motors containing AglR-PAmCherry support gliding motility to the wild type level (Nan *et al*., 2013). We expressed the fusion protein as the sole AglR under its native regulatory control and used single-particle

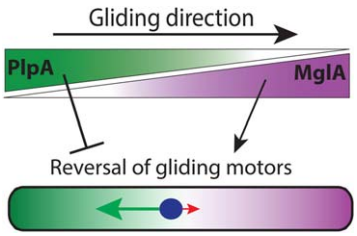

Fig. 8. PlpA regulates the direction of *M. xanthus* gliding motility by antagonizing MglA on individual gliding machineries. The antagonism between PlpA (inhibits motor reversal) and MglA (activates motor reversal) on gliding motors, together with their opposite concentration gradients, stabilize cell polarity during motility. Due to the local concentrations of PlpA and MglA, at nonpolar locations, motors moving toward lagging cell poles (green arrow) are less likely to reverse than those moving toward leading poles (red arrow). Thus, persistent motion of gliding machineries toward lagging cell poles will generate stronger forward propulsion.

tracking photoactivatable localization microscopy (sptPALM) (Manley *et al*., 2008) to map the movements of individual motors by tracking the dynamics of single AglR molecules at 100-ms intervals (Nan *et al*., 2013, 2015). We recorded 212 reversals of AglR particles in 20 cells with wild type gliding motility, normalized cell lengths to 1, and mapped the spatial distribution of these reversals. We found that AglR reversals showed an asymmetric distribution pattern, positively correlating with MglA concentrations ($R^2 = 0.78$) while negatively correlating with PlpA concentrations ($R^2 = 0.81$) (Fig. 7B).

As reported previously, single gliding motors moving in helical tracks along the long axis of cells reverse their direction occasionally, leaving zigzag tracks in kymographs (Fig. 7C) (Nan *et al*., 2015). When PlpA was either absent (in Δ*plpA* cells) or overexpressed (under the control of a vanillate inducible promoter, in the presence of 200 μM sodium vanillate), the velocities of individual motors did not change significantly compared to the wild type (Fig. S12). However, in Δ*plpA* cells, individual motors reversed more frequently, mimicking the phenotype of the MglA overexpression strain (Fig. 7C) (Nan *et al*., 2015). By contrast, when PlpA was overexpressed, individual gliding motors rarely reversed their moving direction, a behavior also observed in Δ*mglA* cells (Nan *et al*., 2015) (Fig. 7C). To quantify the behavior of individual motors, we analyzed the time that individual AglR molecules traveled before reversing. As shown in Fig. 7D, in wild type cells, motors travels for 0.49 ± 0.06 s ($n = 215$) before reversing. In the absence of PlpA, individual motors traveled for less time before reversing (0.26 ± 0.02 s, $n = 291$) (Fig. 7D). By contrast, when PlpA was overexpressed, individual motors traveled for a longer time (0.61 ± 0.06 s, $n = 96$), leaving long and straight tracks in kymographs (Fig. 7D). Taken together, the results of single-particle microscopy

indicate that PlpA regulates cell polarity by inhibiting the reversal of individual gliding motors. Since MglA promotes motor reversal, PlpA appears antagonizing MglA on individual gliding motors.

Discussion

PlpA stabilizes the MglA polarity axis during motility

In this study, we identified a novel regulator, PlpA that controls the directionality of *M. xanthus* motility. Using gliding motility as an indicator, we demonstrated that PlpA antagonizes MglA on individual gliding motors. Due to the opposite asymmetry of MglA and PlpA, the antagonism of PlpA near lagging cell poles will reinforce the function of MglA near the leading poles (Fig. 8).

It is still unclear how regulators such as MglA and PlpA control the moving direction of the entire cell by interacting with individual motility machineries. Here we propose a simple model that provides a potential mechanism. In *M. xanthus* cells, the probability of reversal of gliding motors is regulated by the localized activities of both MglA and PlpA. Thus, due to the opposite concentration gradients of MglA and PlpA, motors moving toward the lagging cell pole are less likely to reverse due to the decreasing MglA concentration and increasing PlpA concentration. By contrast, motors moving toward the leading cell pole are more likely to reverse due to the increasing MglA concentration and decreasing PlpA concentration. Taken together, the net effect of the opposite MglA and PlpA gradients is stronger forward propulsion generated by motors moving toward the lagging cell pole, which would propel cells forward (Fig. 8). This polarity is maintained until the Frz pathway signals an inversion of both gradients (Leonardy *et al.*, 2010; Zhang *et al.*, 2010). This mechanism is analogous to the directional switching of flagella motors during swimming of *E. coli*, in which persistent counterclockwise rotation of flagella motors results in net motion toward attractants or away from repellents.

Our model provides logical explanations for some experimental observations that have previously been difficult to interpret. For example, Cells carrying an *mglB* deletion or expressing the constitutively active MglA variants, $MglA^{Q82L}$ and $MglA^{Q82A}$, feature symmetric bipolar MglA localization (Leonardy *et al.*, 2010; Zhang *et al.*, 2010). If MglA is the only determinant of cell polarity, these cells should not generate any unidirectional movements because both poles are equally polarized. However, as PlpA still remains polarized when the MglA polarity axis diminishes, these cells still move unidirectionally for at lease one cell length before reversing (Zhang *et al.*, 2010). In contrast, when the polarity of both PlpA and MglA are abolished, as in the Δ*mglB* Δ*plpA* cells, the cell polarity axis totally disappears. Accordingly, cells reverse ~ 1.3 times more frequently, resulting in even shorter displacements between reversals (Fig. 2).

It is surprising that RomR largely retains its asymmetric bipolar localization in the absence of PlpA, because PlpA regulates the localization of MglA and MglB (Fig. 5) and both MglA and MglB regulate RomR (Keilberg *et al.*, 2012). Due to its lack of direct interaction with the Mgl module (Supporting Information Fig. S7), PlpA is not likely to regulate the activities of MglA and MglB. We hypothesize that the correct localization of RomR might require both the localization and catalytic activities of MglA and MglB. If this hypothesis is true, since the activities of MglA and MglB are still intact, the absence of PlpA only causes limited changes in the localization of RomR (Fig. 5). However, significantly more data are required to prove this hypothesis.

The regulatory similarities between gliding and swimming

As mentioned previously, PlpA is conserved in the order of *Myxococcales* where the flagella stator homologues AglR/Q/S are reconfigured as motors for surface motility (Luciano *et al.*, 2011). Besides the fundamental similarity between the energy-harvesting units (*M. xanthus* AglR/Q/S and *E. coli* MotA/B are homologous proton channels), gliding and flagella-powered swimming also share similarities in regulation. In both cases, the signaling cascades that control the moving direction of cells start from chemotaxis pathways, the Che system in *E. coli* and the Frz system in *M. xanthus* (Zusman *et al.*, 2007). The identification of PlpA adds yet another layer of similarity between these two motility systems. PilZ-like proteins regulate flagella assembly and rotation during swimming and swarming in other species similar to *M. xanthus* PlpA. For example, the *E. coli* PilZ-like protein YcgR functions as a molecular break that fine-tunes flagella rotation through direct interactions with MotA in the stator and/or FliG/M in the flagellum switch complex (Boehm *et al.*, 2010; Fang and Gomelsky, 2010, Paul *et al.*, 2010). In *P. aeruginosa*, FlgZ directly interacts with stator protein MotC, enabling cells to quickly adapt to changing environmental conditions (Baker *et al.*, 2016). These striking similarities suggest that PlpA and the AglR/Q/S motor might have coevolved in myxobacteria and are specifically reconfigured for gliding.

Although PlpA assembles into the motility machinery, it rarely forms clusters. Instead, the nonpolar PlpA clusters observed in about 5% cells might indicate concentrated PlpA activities that are not regularly observed in cells. In this study, we took advantage of those nonpolar

Table 1. *M. xanthus* strains used in this study.

Strains	Genotype	Reference source
DZ2	Wild type	(Campos *et al.*, 1978)
DZ4469	*pilA::tet*	(Vlamakis *et al.*, 2004)
DZ4486	*frzCD*^{c} (*frzCD*$^{\Delta 6-153}$)	(Bustamante *et al.*, 2004)
DZ4481	Δ*frzE*	(Bustamante *et al.*, 2004)
DZ4484	Δ*frzZ*	(Bustamante *et al.*, 2004)
DZ4833	*frzZ-gfp*	(Kaimer and Zusman, 2013)
TM12	Δ*mglA*	(Zhang *et al.*, 2010)
TM155	Δ*mglB*	(Zhang *et al.*, 2010)
TM254	Δ*romR*	(Zhang *et al.*, 2012)
TM3	*frzS-gfp*	(Mignot *et al.*, 2005)
BN120	Δ*aglR pilA::tet*	(Nan *et al.*, 2011)
BN121	Δ*aglQS*	This study
BN200	*aglR-PAmCherry*	(Nan *et al.*, 2013)
BN201	Δ*plpA*	This study
BN202	*plpA*^{R15D}	This study
BN203	*plpA*^{R15D} *pilA::tet*	This study
BN204	*plpA*^{S39A}	This study
BN205	*plpA*^{S39A} *pilA::tet*	This study
BN206	*plpA*$^{G41A\ G42A}$	This study
BN207	*plpA*$^{G41A\ G42A}$ *pilA::tet*	This study
BN208	Δ*plpA pilA::tet*	This study
BN209	*plpA-gfp*	This study
BN210	*plpA*^{R15D}*-gfp*	This study
BN211	*plpA*^{S39A}*-gfp*	This study
BN212	*plpA*$^{G41A\ G42A}$*-gfp*	This study
BN213	*plpA-gfp pilA::tet*	This study
BN214	*pMR3679-plpA*	This study
BN215	*pMR3679-plpA pilA::tet*	This study
BN216	Δ*mglC*	This study
BN217	Δ*frzE pilA::tet*	This study
BN218	*frzCD*^{c} (*frzCD*$^{\Delta 6-153}$) *pilA::tet*	This study
BN219	Δ*mglC pilA::tet*	This study
BN220	Δ*mglA pilA::tet*	This study
BN221	Δ*mglB pilA::tet*	This study
BN222	Δ*romR pilA::tet*	This study
BN223	Δ*plpA* Δ*mglA*	This study
BN224	Δ*plpA* Δ*mglA pSWU19-mglB-yfp*	This study
BN225	Δ*plpA* Δ*mglA pilA::tet*	This study
BN226	Δ*plpA* Δ*mglB*	This study
BN227	Δ*plpA* Δ*mglB pMR3562-mglA-mCherry*	This study
BN228	Δ*plpA* Δ*mglB pilA::tet*	This study
BN229	Δ*plpA* Δ*romR*	This study
BN230	Δ*plpA* Δ*romR pilA::tet*	This study
BN231	Δ*plpA* Δ*mglC*	This study
BN232	Δ*plpA* Δ*mglC pilA::tet*	This study
BN233	*frzCD*^{c} Δ*plpA*	This study
BN234	*frzCD*^{c} *pMR3679-plpA*	This study
BN235	*frzCD*^{c} *pMR3679-plpA pilA::tet*	This study
BN236	Δ*frzE* Δ*plpA*	This study
BN237	Δ*frzE* Δ*plpA pilA::tet*	This study
BN238	*frzCD*^{c} Δ*plpA pilA::tet*	This study
BN239	Δ*plpA pMR3562-mglA-mCherry*	This study
BN240	Δ*plpA pSWU19-mglB-yfp*	This study
BN241	Δ*plpA pMR3562-romR-yfp*	This study
BN242	Δ*plpA* Δ*mglA pMR3562-romR-yfp*	This study
BN243	Δ*plpA* Δ*mglB pMR3562-romR-yfp*	This study
BN244	Δ*plpA pSWU19-mglC-mCherry*	This study
BN245	Δ*plpA frzZ-gfp*	This study
BN246	Δ*plpA frzS-gfp*	This study
BN247	Δ*aglQS plpA-gfp*	This study
BN248	Δ*mglA plpA-gfp*	This study
BN249	Δ*mglB plpA-gfp*	This study
BN267	Δ*mglC plpA-gfp*	This study
BN268	Δ*romR plpA-gfp*	This study
BN269	Δ*frzZ plpA-gfp*	This study
BN270	*plpA-gfp pMR3629-mglA*	This study

Table 1: *Continued*

Strains	Genotype	Reference source
BN271	*plpA-gfp pMR3629-mglB*	This study
BN272	*pSWU19-mglC-mCherry*	This study
BN273	*ΔplpA pSWU19-mglC-mCherry*	This study
BN274	*plpA-gfp pMR3629-mglC*	This study
BN275	*plpA-gfp pMR3562-romR*	This study
BN276	*ΔplpA aglR-PAmCherry*	This study
BN277	*aglR-PAmCherry pMR3679-plpA*	This study
BN278	*ΔaglQS ΔplpA*	This study
BN279	*plpA-gfp pSWU30-mglA*^{Q82L}	This study
BN280	*plpA-gfp pMR3562-mglA-mCherry*	This study
BN281	*pMR3562-mglA-mCherry*	This study
BN282	*pSWU19-mglB-yfp*	This study
BN283	*pMR3562-romR-yfp*	This study
BN284	*plpA-gfp agmU (gltD)-mCherry*	This study

PlpA clusters to show their colocalization with the gliding machinery. A comparable example is MglA, which has been proved to assemble into the gliding machinery (Treuner-Lange *et al*., 2015). Similar to PlpA, MglA does not form nonpolar clusters regularly. Instead, nonpolar clusters were only observed in ∼ 50% of cells that express a YFP-labeled MglA variant, MglA^{Q82A} (similar to MglA^{Q82L} used in this study) (Treuner-Lange *et al*., 2015), which locks MglA to the GTP-bound conformation (Zhang *et al*., 2010; Miertzschke *et al*., 2011). Much remains to be understood about the mechanisms by which small regulators, such as PlpA and MglA assemble into the gliding machinery.

Experimental procedures

BACTH screening and pairwise BACTH assay

A *M. xanthus* DNA library was constructed using Phenol/chloroform-extracted chromosomal DNA. Briefly, *M. xanthus* DZ2 cells were grown to $OD_{600} = 1$. Cells were collected by centrifugation and re-suspended in 800 μl H_2O before subjected to sonication. Chromosomal DNA was then purified using the Phenol/chloroform extraction method (Sambrook and Russell, 2001). The resulted DNA was fragmented using fragmentase (New England Biolabs) at 37°C for 1–15 min. To stop the reaction, samples were incubated at 65°C for 10 min, with 25 mM EDTA and 50 mM DTT added. The end repair of the DNA fragments was performed at 20°C for 20 min in a 100 μl reaction containing 7.5 μg DNA, 10 μl T4 Ligase Buffer (10×), 5 μl dNTPs (2 mM each), 5 μl T4 DNA Polymerase, 1 μl Klenow Fragment and 5 μl Polynucleotide Kinase. The resulted DNA was purified and checked using agarose electrophoresis (Sambrook and Russell, 2001). Fragments between 300 and 1500 bp were cut from the gel, purified and ligated into the pKT25 vector (Karimova *et al*., 1998) using the *Sma*I restriction site. The ligation product was purified and co-transformed into MAX efficiency™ DH5α competent cells (Thermo Fisher) together with pUT18-*aglS* using heat shock method (Sambrook and Russell, 2001). Cells were incubated at 37°C for 1 h, washed twice with M63 medium (Sambrook and Russell, 2001) and plated on M63 solid medium containing 0.2% maltose, 50 μg ml^{-1} ampicillin, 25 μg ml^{-1} kanamycin, 40 μg ml^{-1} X-Gal and 0.5 mM IPTG. Blue colonies were selected, the pKT25 plasmids were purified, and proteins potentially interacting with AglS were identified by DNA sequencing using the pKT25 forward primer. Pairwise BACTH assays were performed using the previously described method (Karimova *et al*., 1998; Nan *et al*., 2015). Primers used for plasmid construction are listed in Supporting Information Table S1.

Expression, purification, denaturation and refolding of PlpA

The DNA sequence encoding PlpA was cloned into the pET30a vector (Novagen) using the primers listed in Supporting Information Table S1. The expression of PlpA was induced by 0.5 mM IPTG at 16°C for 10 h in the *E. coli* strain BL21 (DE3). The purification, denaturation and refolding of PlpA was performed using the methods described in (Zhou *et al*., 2008; Nan *et al*., 2010a). Briefly, transformed *E. coli* BL21 (DE3) cells were cultured in 20 ml LB (Luria-Bertani) broth at 37°C overnight and used to inoculate 1 l medium which contains 1.5% (w/v) Bacto Tryptone (BD Biosciences), 1% Bacto yeast extract and 5 g l^{-1}. Expression of the recombinant protein was induced by 0.5 mM IPTG (isopropyl-h-d-thiogalactopyranoside) when the culture reached an OD_{600} of 0.8. Cultivation was continued at 16°C for 10 h before the cells were harvested by centrifugation at 8000 rpm for 10 min. The pellet was suspended in buffer A (20 mM Tris–HCl pH 8.0, 500 mM NaCl) and the cells were lysed by sonication on ice. The lysate was centrifuged twice (18 000 rpm, 4°C, 30 min) to remove debris prior to the purification procedure using a 5-ml Hitrap Ni^{2+} chelating column and FPLC (GE Healthcare). Recombinant PlpA protein was eluted using buffer B (20 mM Tris–HCl pH 8.0, 500 mM NaCl, 200 mM imidazole) and directly concentrated using a Millipore centrifugal filter device with a 3 kDa cut-off. To eliminate the excess imidazole, the protein solution was diluted in buffer A and concentrated for five times (Nan *et al*., 2006). Purified protein was stored at −80°C.

ITC assay

ITC assays were performed using a MicroCal™ iTC200 isothermal titration calorimeter (Malvern), following previous described procedures (Nan *et al.*, 2010a), except for that the concentrations of PlpA (both natively purified and refolded) and c-di-GMP (Axxora) were 10 μM and 100 μM respectively. c-di-GMP was diluted into buffer A to a concentration of 100 μM at 25°C and injected into the sample chamber containing 10 μM PlpA solution. ITC titrations were performed at 25°C.

Strains and growth conditions

M. xanthus strains used in this study are listed in Table 1. Motility and reversal frequency assays were performed using the same methods described in (Bustamante *et al.*, 2004; Mauriello *et al.*, 2009; Nan *et al.*, 2010b). To determine cell reversal frequency, cells were grown in liquid CYE medium, which contains 10 mM MOPS pH 7.6, 1% (w/v) Bacto Casitone (BD Biosciences), 0.5% Bacto yeast extract and 4 mM $MgSO_4$ (Campos *et al.*, 1978) and spotted on a thin fresh 0.5 CTT agar (Wu and Kaiser, 1997).

Deletion, point mutation and insertion mutants were constructed by electroporating *M. xanthus* cells with 4 μg of plasmid DNA or 1 μg of chromosomal DNA. Transformed cells were plated on CYE plates supplemented with 100 mg ml^{-1} sodium kanamycin sulfate. Site-directed mutagenesis of the *plpA* gene was performed using PCR method using the wild type *plpA* gene as templates (Sambrook and Russell, 2001). To construct the in-frame deletion or point mutation strains, in-frame deletion or point mutation cassettes were amplified with polymerase chain reaction (PCR) using chromosomal DNA as template, digested and inserted into plasmid pBJ113. All constructs were confirmed by DNA sequencing. Transformants were obtained by homologous recombination as previously described (Bustamante *et al.*, 2004). The primers used in the constructions of the in-frame deletions and insertions are summarized in Supporting Information Table S1.

Microscopy

Time-lapse videos were recorded with a ZEISS AXIO™ microscope and a ZEISS AxioCam™ MRm camera at 10-s intervals. The reversals from 40 individual cells within 20 min were counted and analyzed. Colony morphology was recorded using a ZEISS SteREO™ microscope and a ZEISS AxioCam™ HSm camera. Fluorescence microscopy, sptPALM and data analysis were performed as described in (Nan *et al.*, 2011, 2013). Microscopy images and time-lapses were captured using a Hamamatsu ImagEM X2™ EM-CCD camera C9100-23B (pixel size 160 nm) on an inverted Nikon Eclipse-Ti microscope with a 100× 1.49 NA TIRF objective.

Acknowledgements

The authors thank Prof. David Zusman for his continuous support in research, helpful discussion and critical reading of this manuscript. We thank Dr. Christine Kaimer for providing technical advices and the help on DNA library construction and Im-Hong Sun for the initial BACTH screening. We thank Prof. Jennifer Doudna and Dr. Ross Wilson for their help on ITC assays. Our research is supported by a Texas A&M University Startup funding.

References

Alm, R.A., Bodero, A.J., Free, P.D., and Mattick, J.S. (1996) Identification of a novel gene, *pilZ*, essential for type 4 fimbrial biogenesis in *Pseudomonas aeruginosa*. *J Bacteriol* **178**: 46–53.

Amikam, D., and Galperin, M.Y. (2006) PilZ domain is part of the bacterial c-di-GMP binding protein. *Bioinformatics* **22**: 3–6.

Baker, A.E., Diepold, A., Kuchma, S.L., Scott, J.E., Ha, D.G., Orazi, G., *et al.* (2016) PilZ domain protein FlgZ mediates cyclic Di-GMP-dependent swarming motility control in *Pseudomonas aeruginosa*. *J Bacteriol* **198**: 1837–1846.

Berleman, J.E., Vicente, J.J., Davis, A.E., Jiang, S.Y., Seo, Y.-E., Zusman, D.R., and Driks, A. (2011) FrzS regulates social motility in *Myxococcus xanthus* by controlling exopolysaccharide production. *PLoS One* **6**: e23920.

Boehm, A., Kaiser, M., Li, H., Spangler, C., Kasper, C.A., Ackermann, M., *et al.* (2010) Second messenger-mediated adjustment of bacterial swimming velocity. *Cell* **141**: 107–116.

Bulyha, I., Lindow, S., Lin, L., Bolte, K., Wuichet, K., Kahnt, J., *et al.* (2013) Two small GTPases act in concert with the bactofilin cytoskeleton to regulate dynamic bacterial cell polarity. *Dev Cell* **25**: 119–131.

Bustamante, V.H., Martinez-Flores, I., Vlamakis, H.C., and Zusman, D.R. (2004) Analysis of the Frz signal transduction system of *Myxococcus xanthus* shows the importance of the conserved C-terminal region of the cytoplasmic chemoreceptor FrzCD in sensing signals. *Mol Microbiol* **53**: 1501–1513.

Campos, J.M., Geisselsoder, J., and Zusman, D.R. (1978) Isolation of bacteriophage MX4, a generalized transducing phage for *Myxococcus xanthus*. *J Mol Biol* **119**: 167–178.

Chang, Y.W., Rettberg, L., Treuner-Lange, A., Iwasa, A., Sogaard-Andersen, J.L., and Jensen, G.J. (2016) Architecture of the type IVa pilus machine. *Science* **351**: aad2001.

Fang, X., and Gomelsky, M. (2010) A post-translational, c-di-GMP-dependent mechanism regulating flagellar motility. *Mol Microbiol* **76**: 1295–1305.

Faure, L.M., Fiche, J.B., Espinosa, L., Ducret, A., Anantharaman, V., Luciano, J., *et al.* (2016) The mechanism of force transmission at bacterial focal adhesion complexes. *Nature* **539**: 530–535.

Guzzo, M., Agrebi, R., Espinosa, L., Baronian, G., Molle, V., Mauriello, E.M.F., *et al.* (2015) Evolution and design governing signal precision and amplification in a bacterial chemosensory pathway. *PLoS Genet* **11**: e1005460.

Hallberg, Z.F., Wang, X.C., Wright, T.A., Nan, B., Ad, O., Yeo, J., and Hammond, M.C. (2016) Hybrid promiscuous

(Hypr) GGDEF enzymes produce cyclic AMP-GMP (3', 3'-cGAMP). *Proc Natl Acad Sci U S A* **113**: 1790–1795.

Hengge, R. (2009) Principles of c-di-GMP signalling in bacteria. *Nat Rev Microbiol* **7**: 263–273.

Hodgkin, J., and Kaiser, D. (1979) Genetics of gliding motility in *Myxococcus xanthus* (Myxobacterales): two gene systems control movement. *Mol Gen Genet* **171**: 177–191.

Huntley, S., Hamann, N., Wegener-Feldbrugge, S., Treuner-Lange, A., Kube, M., Reinhardt, R., *et al*. (2011) Comparative genomic analysis of fruiting body formation in *Myxococcales*. *Mol Biol Evol* **28**: 1083–1097.

Iniesta, A.A., Garcia-Heras, F., Abellon-Ruiz, J., Gallego-Garcia, A., and Elias-Arnanz, M. (2012) Two systems for conditional gene expression in *Myxococcus xanthus* inducible by isopropyl-beta-D-thiogalactopyranoside or vanillate. *J Bacteriol* **194**: 5875–5885.

Jenal, U., and Malone, J. (2006) Mechanisms of cyclic-di-GMP signaling in bacteria. *Annu Rev Genet* **40**: 385–407.

Kaimer, C., and Zusman, D.R. (2013) Phosphorylation-dependent localization of the response regulator FrzZ signals cell reversals in *Myxococcus xanthus*. *Mol Microbiol* **88**: 740–753.

Kaimer, C., and Zusman, D.R. (2016) Regulation of cell reversal frequency in *Myxococcus xanthus* requires the balanced activity of CheY-like domains in FrzE and FrzZ. *Mol Microbiol* **100**: 379–395.s

Kaimer, C., Berleman, J.E., and Zusman, D.R. (2012) Chemosensory signaling controls motility and subcellular polarity in *Myxococcus xanthus*. *Curr Opin Microbiol* **15**: 751–757.

Karimova, G., Pidoux, J., Ullmann, A., and Ladant, D. (1998) A bacterial two-hybrid system based on a reconstituted signal transduction pathway. *Proc Natl Acad Sci U S A* **95**: 5752–5756.

Keilberg, D., Wuichet, K., Drescher, F., Søgaard-Andersen, L., and Viollier, P.H. (2012) A response regulator interfaces between the Frz chemosensory system and the MglA/MglB GTPase/GAP module to regulate polarity in *Myxococcus xanthus*. *PLoS Genet* **8**: e1002951.

Lenz, P., and Sogaard-Andersen, L. (2011) Temporal and spatial oscillations in bacteria. *Nat Rev Microbiol* **9**: 565–577.

Leonardy, S., Freymark, G., Hebener, S., Ellehauge, E., and Sogaard-Andersen, L. (2007) Coupling of protein localization and cell movements by a dynamically localized response regulator in *Myxococcus xanthus*. *EMBO J* **26**: 4433–4444.

Leonardy, S., Miertzschke, M., Bulyha, I., Sperling, E., Wittinghofer, A., and Sogaard-Andersen, L. (2010) Regulation of dynamic polarity switching in bacteria by a Ras-like G-protein and its cognate GAP. *EMBO J* **29**: 2276–2289.

Luciano, J., Agrebi, R., Le Gall, A.V., Wartel, M., Fiegna, F., Ducret, A., *et al*. (2011) Emergence and modular evolution of a novel motility machinery in bacteria. *PLoS Genet* **7**: e1002268.

Manley, S., Gillette, J.M., Patterson, G.H., Shroff, H., Hess, H.F., Betzig, E., and Lippincott-Schwartz, J. (2008) High-density mapping of single-molecule trajectories with photoactivated localization microscopy. *Nat Methods* **5**: 155–157.

Mauriello, E.M., Mouhamar, F., Nan, B., Ducret, A., Dai, D., Zusman, D.R., and Mignot, T. (2010) Bacterial motility complexes require the actin-like protein, MreB and the Ras homologue, MglA. *EMBO J* **29**: 315–326.

Mauriello, E.M.F., Nan, B., and Zusman, D.R. (2009) AglZ regulates adventurous (A-) motility in *Myxococcus xanthus* through its interaction with the cytoplasmic receptor, FrzCD. *Mol Microbiol* **72**: 964–977.

McLoon, A.L., Wuichet, K., Hasler, M., Keilberg, D., Szadkowski, D., and Sogaard-Andersen, L. (2015) MglC, a paralog of *Myxococcus xanthus* GTPase activating protein MglB, plays a divergent role in motility regulation. *J Bacteriol* **198**: 510–520.

Miertzschke, M., Koerner, C., Vetter, I.R., Keilberg, D., Hot, E., Leonardy, S., *et al*. (2011) Structural analysis of the Ras-like G protein MglA and its cognate GAP MglB and implications for bacterial polarity. *EMBO J* **30**: 4185–4197.

Mignot, T., Merlie, J., and Zusman, D. (2005) Regulated pole-to-pole oscillations of a bacterial gliding motility protein. *Science* **310**: 855–857.

Muller, F.D., Treuner-Lange, A., Heider, J., Huntley, S.M., and Higgs, P.I. (2010) Global transcriptome analysis of spore formation in *Myxococcus xanthus* reveals a locus necessary for cell differentiation. *BMC Genomics* **11**: 264.

Muñoz-Dorado, J., Marcos-Torres, F.J., García-Bravo, E., Moraleda-Muñoz, A., and Pérez, J. (2016) Myxobacteria: moving, killing, feeding, and surviving together. *Front Microbiol* **7**: 781.

Nan, B., and Zusman, D.R. (2016) Novel mechanisms power bacterial gliding motility. *Mol Microbiol* **101**: 186–193.

Nan, B., Zhou, Y., Liang, Y.H., Wen, J., Ma, Q., Zhang, S., *et al*. (2006) Purification and preliminary X-ray crystallographic analysis of the ligand-binding domain of *Sinorhizobium meliloti* DctB. *Biochim Biophys Acta* **1764**: 839–841.

Nan, B., Liu, X., Zhou, Y., Liu, J., Zhang, L., Wen, J., *et al*. (2010a) From signal perception to signal transduction: ligand-induced dimeric switch of DctB sensory domain in solution. *Mol Microbiol* **75**: 1484–1494.

Nan, B., Mauriello, E.M., Sun, I.H., Wong, A., and Zusman, D.R. (2010b) A multi-protein complex from *Myxococcus xanthus* required for bacterial gliding motility. *Mol Microbiol* **76**: 1539–1554.

Nan, B., Chen, J., Neu, J.C., Berry, R.M., Oster, G., and Zusman, D.R. (2011) Myxobacteria gliding motility requires cytoskeleton rotation powered by proton motive force. *Proc Natl Acad Sci U S A* **108**: 2498–2503.

Nan, B., Bandaria, J.N., Moghtaderi, A., Sun, I.H., Yildiz, A., and Zusman, D.R. (2013) Flagella stator homologs function as motors for myxobacterial gliding motility by moving in helical trajectories. *Proc Natl Acad Sci U S A* **110**: E1508–E1513.

Nan, B., McBride, M.J., Chen, J., Zusman, D.R., and Oster, G. (2014) Bacteria that glide with helical tracks. *Curr Biol* **24**: R169–R173.

Nan, B., Bandaria, J.N., Guo, K.Y., Fan, X., Moghtaderi, A., Yildiz, A., and Zusman, D.R. (2015) The polarity of myxobacterial gliding is regulated by direct interactions between the gliding motors and the Ras homolog MglA. *Proc Natl Acad Sci U S A* **112**: E186–E193.

Paul, K., Nieto, V., Carlquist, W.C., Blair, D.F., and Harshey, R.M. (2010) The c-di-GMP binding protein YcgR controls flagellar motor direction and speed to affect chemotaxis by a "backstop brake" mechanism. *Mol Cell* **38**: 128–139.

Ryjenkov, D.A., Simm, R., Romling, U., and Gomelsky, M. (2006) The PilZ domain is a receptor for the second messenger c-di-GMP: the PilZ domain protein YcgR controls motility in enterobacteria. *J Biol Chem* **281**: 30310–30314.

Sambrook, J., and Russell, D.W. (2001) *Molecular Cloning: A Laboratory Manual 3rd Edition. Chapter 18: Protein Interaction Technologies, Protocol #3: Detection of Protein-Protein Interactions Using the GST Fusion Protein Pull-down Technique*. Plainview, NY: Cold Spring Harbor Laboratory Press.

Schumacher, D., and Sogaard-Andersen, L. (2017) Regulation of cell polarity in motility and cell division in *Myxococcus xanthus*. *Annu Rev Microbiol* **71**: 61–78.

Shi, W., and Zusman, D.R. (1993) The two motility systems of *Myxococcus xanthus* show different selective advantages on various surfaces. *Proc Natl Acad Sci U S A* **90**: 3378–3382.

Skotnicka, D., Petters, T., Heering, J., Hoppert, M., Kaever, V., and Sogaard-Andersen, L. (2016a) Cyclic Di-GMP regulates type IV Pilus-dependent motility in *Myxococcus xanthus*. *J Bacteriol* **198**: 77–90.

Skotnicka, D., Smaldone, G., Petters, T., Trampari, T., Liang, E., Kaever, J.V., *et al*. (2016b) A minimal threshold of c-di-GMP is essential for fruiting body formation and sporulation in *Myxococcus xanthus*. *PLoS Genet* **12**: e1006080.

Sun, H., Zusman, D.R., and Shi, W. (2000) Type IV pilus of *Myxococcus xanthus* is a motility apparatus controlled by the *frz* chemosensory system. *Curr Biol* **10**: 1143–1146.

Sun, M., Wartel, M., Cascales, E., Shaevitz, J.W., and Mignot, T. (2011) Motor-driven intracellular transport powers bacterial gliding motility. *Proc Natl Acad Sci U S A* **108**: 7559–7564.

Treuner-Lange, A., and Sogaard-Andersen, L. (2014) Regulation of cell polarity in bacteria. *J Cell Biol* **206**: 7–17.

Treuner-Lange, A., Macia, E., Guzzo, M., Hot, E., Faure, L.M., Jakobczak, B., *et al*. (2015) The small G-protein MglA connects to the MreB actin cytoskeleton at bacterial focal adhesions. *J Cell Biol* **210**: 243–256.

Vlamakis, H.C., Kirby, J.R., and Zusman, D.R. (2004) The Che4 pathway of *Myxococcus xanthus* regulates type IV pilus-mediated motility. *Mol Microbiol* **52**: 1799–1811.

Wu, S.S., and Kaiser, D. (1997) Regulation of expression of the *pilA* gene in *Myxococcus xanthus*. *J Bacteriol* **179**: 7748–7758.

Wu, Y., Kaiser, A.D., Jiang, Y., and Alber, M.S. (2009) Periodic reversal of direction allows Myxobacteria to swarm. *Proc Natl Acad Sci* **106**: 1222–1227.

Zhang, Y., Franco, M., Ducret, A., Mignot, T., and Laub, M.T. (2010) A bacterial Ras-like small GTP-binding protein and its cognate GAP establish a dynamic spatial polarity axis to control directed motility. *PLoS Biol* **8**: e1000430.

Zhang, Y., Guzzo, M., Ducret, A., Li, Y.-Z., Mignot, T., and Viollier, P.H. (2012) A dynamic response regulator protein modulates G-protein-dependent polarity in the bacterium *Myxococcus xanthus*. *PLoS Genet* **8**: e1002872.

Zhou, T., and Nan, B. (2017) Exopolysaccharides promote *Myxococcus xanthus* social motility by inhibiting cellular reversals. *Mol Microbiol* **103**: 729–743.

Zhou, Y.F., Nan, B., Nan, J., Ma, Q., Panjikar, S., Liang, Y.H., *et al*. (2008) C4-dicarboxylates sensing mechanism revealed by the crystal structures of DctB sensor domain. *J Mol Biol* **383**: 49–61.

Zusman, D.R., Scott, A.E., Yang, Z., and Kirby, J.R. (2007) Chemosensory pathways, motility and development in *Myxococcus xanthus*. *Nat Rev Microbiol* **5**: 862–872.

Supporting information

Additional supporting information may be found in the online version of this article at the publisher's web-site.